Nondestructive Evaluation of Buried Dielectric Cylinders by Asynchronous Particle Swarm Optimization

Wei-Tsong Lee[1], Chi-Hsien Sun[2], Chien-Ching Chiu[1] and

Jyun-Fu Li[1]

[1]Electrical Engineering Department, Tamkang University

Tamsui, Taiwan, R.O.C.

[2]Department of Electronic and Computer Engineering, National Taiwan University of Science and Technology, Taipei City, Taiwan, R.O.C.

Abstract

This paper presents the studies of time domain inverse scattering for a two dimensional inhomogeneous dielectric cylinder buried in a slab medium by the finite difference time domain (FDTD) method and the asynchronous particle swarm optimization (APSO) method. For the forward scattering part, the FDTD method is employed to calculate the scattered E fields. Base on the scattering fields, these inverse scattering problems are transformed into optimization problems. The APSO is applied to reconstruct permittivity of the two-dimensional inhomogeneous dielectric cylinder. In addition, the effects of Gaussian noise on the reconstruction results are investigated. Numerical results show that even when the measured scattered fields are contaminated with Gaussian noise, APSO ten times is able to yield good reconstructed quality.

Index Terms– FDTD, asynchronous particle swarm optimization

(APSO), inhomogeneous dielectric cylinders, time domain inverse scattering

I. INTRODUCTION

The objective of the inverse problem is to determine the electromagnetic properties of the buried scatterer from the scattered field measured outside. There are many applications such as geophysical prospecting, medical imaging, non-destructive evaluated, determination of underground tunnels and pipelines, etc [1]-[10]. However, it is well known that one major difficulty of inverse scattering is its nonlinearity because it involves the product of two unknowns: the electrical properties of object, and the electric field within the object [11].

In general, the nonlinearity of the problem is coped with by applying iterative optimization techniques, concretely two techniques are employed. The first is traditional deterministic methods, such as Born iterative method (BIM) [12] and the distorted Born iterative method (DBIM) [13]. Furthermore, for a gradient-type method, it is well known that the convergence of the iteration depends highly on the initial guess. If a good initial guess is given, the speed of the convergence can be very fast. On the other hand, if the initial guess is far away from the exact one, searching tends to get fail [14].

The second is stochastic methods. These algorithms based on strategies offer advantages relative to local inversion algorithms including strong search ability, simplicity, robustness and insensitivity to nonlinearity. In contrast to traditional deterministic methods, evolutionary searching schemes provide a more robust and efficient approach for solving inverse

scattering problems [15]-[17]. Thus, some stochastic methods, such as genetic algorithm (GA) [18]-[21], particle swarm optimization (PSO) [22]-[26], differential evolution/dynamic differential evolution (DE/DDE) [17], [26]-[34] are proposed to search the global extreme of the inverse problems to overcome the drawback of the deterministic methods. However, these papers only focus on homogeneous dielectric cylinder or perfectly conducting cylinder cases.

Recently, there are a few reports on this subject of 2-D object about inhomogeneous dielectric cylinder under time domain [32]-[34]. The reference [33] focuses on two-dimensional inhomogeneous dielectric cylinder buried in a half-space by using dynamic differential evolution (DDE) and non-uniform steady state genetic algorithm (NU-SSGA). To the best of our knowledge, there is still no investigation on using the APSO to reconstruct the electromagnetic imaging of inhomogeneous dielectric cylinders with arbitrary cross section in a three-layered slab medium under time domain.

This paper presents a time domain computational scheme for the microwave imaging of a 2D inhomogeneous dielectric cylinder. The forward problem is solved by the FDTD method. The inverse problem is formulated into an optimization problem, and then the global searching scheme APSO is used to search the parameter space. In Section II, the theoretical formulation for the electromagnetic imaging is presented. The general principle of the APSO scheme and the way we applied it to the imaging problem are described. In section III, some numerical results are presented. Finally, in section IV some conclusions are drawn.

II. THEORETICAL FORMULATION

Consider a 2-D inhomogeneous dielectric cylinder buried in a slab medium material medium as shown in Figure 1. The cylinder is parallel to z axis buried between the planar interfaces separating three homogeneous spaces: the region 1 (ε_1, μ_1), the region 2 (ε_2, μ_2) and region 3 (ε_1, μ_2). The permittivity of the buried dielectric object is denoted by $\varepsilon_3(x, y)$. The dielectric object is illuminated by a Gaussian pulse line source located at the points denoted by $\mathrm{T_x}$ in the first layer and scattered waves are recorded at those points denoted by $\mathrm{R_x}$ in the same layer. The computational domain is surrounded by the perfect matching layers (PML) absorber [35] to reduce the reflection from the environment-PML interface.

A. Forward Problem

The direct scattering problem is to calculate the scattered electric fields for a given permittivity ε_3 . The scatterer region is subdivided by a rectangular grid with R and U subdivisions along the x and y axis, respectively. Then, the relative permittivity is expressed as

$$\varepsilon_3(x, y) = \sum_{r=1}^{R} \sum_{u=1}^{U} \alpha_{ru} II_{ru}(x, y) \tag{1}$$

where

$$II_{ru}(x,y)=\begin{cases}1 \text{ if } (x,y) \in [x_r, x_{r+1}] \times [y_u, y_{u+1}] \\ 0 \text{ elsewhere}\end{cases} \tag{2}$$

are the pulse functions.

B. Inverse Problem

For the inverse scattering problem, the permittivity of the dielectric cylinder is reconstructed through the given scattered electric fields obtained at the receivers. This problem is formulated as an optimization problem, for which the global searching scheme APSO is employed to minimize the following objective function (*OF*):

$$OF = \frac{\sum_{n=1}^{N_i}\sum_{m=1}^{M}\sum_{k=0}^{K}\left|E_z^{\exp}(n,m,k\Delta t) - E_z^{cal}(n,m,k\Delta t)\right|}{\sum_{n=1}^{N_i}\sum_{m=1}^{M}\sum_{k=0}^{K}\left|E_z^{\exp}(n,m,k\Delta t)\right|} \tag{3}$$

where $E_z^{\exp}$ and E_z^{cal} are the experimental electric fields and calculated electric fields, respectively. The N_i and M are the total number of the transmitters and receivers, respectively. K is the total time step number of the recorded electric fields.

C. Asynchronous Particle Swarm Optimization (APSO)

Particle swarm global optimization is a class of derivative-free, population-based and self-adaptive search optimization technique which was introduced by Kennedy and Eberhart [36]. PSO has proven to be a useful method of optimization for difficult and discontinuous multidimensional engineering problems [37]-[39] due to its efficiency of exploring the entire search space.

Particles (potential solutions) are distributed throughout the searching

space and their positions and velocities are modified based on social behavior. The social behaviors in PSO exhibit a population of particles moving toward the most promising region of the search space. Clerc [40] proposed the constriction factor to adjust the velocity of the particle for obtaining the better convergence; the algorithm was named as constriction factor method (CFM). PSO starts with an initial population of potential solutions that is randomly generated and composed of N_p individuals (also called particles), of which each represents the permittivity distribution of the cylinder.

After the initialization step, each particle of population is associated with a randomized velocity and position. Thus, each particle has a position and velocity vector, and can move through the problem space. In each generation, the particle changes its velocity according to its best experience, called x_{pbest}, and the best particle in the swarm, called x_{gbest}.

Assume there are N_p particles in the swarm that is in a search space of D dimensions, the position and velocity of the i-th particle is determined according to the constriction factor method as follows:

$$v_{id}^{k} = \chi \cdot \left(v_{id}^{k-1} + c_1 \cdot \varphi_1 \cdot \left(x_{pbest,\,id} - x_{id}^{k-1} \right) + c_2 \cdot \varphi_2 \cdot \left(x_{gbest,\,id} - x_{id}^{k-1} \right) \right) \quad (4)$$

$$x_{id}^{k} = x_{id}^{k-1} + v_{id}^{k} \quad (5)$$

where $\chi = \dfrac{2}{\left| 2 - \phi - \sqrt{\phi^2 - 4\phi} \right|}$, $\phi = c_1 + c_2 \geq 4$. c_1 and c_2 are the learning coefficients used to control the impact of the local and global component in velocity equation (4). v_{id}^{k} and x_{id}^{k} are the velocity and position of the

i-th particle with *d*-th dimension at the *k*-th generation, φ_1 and φ_2 are both random numbers between 0 and 1.

Asynchronous PSO use the following rule: after each particle position updates if the new best position is better than the current best position, the new best position will replace the current best position and be used in the next particles swarm immediately. In this way, the swarm reacts more quickly to speedup the convergence because the updating occurs immediately after cost function evaluation for each particle.

The “damping boundary condition” was proposed by Huang and Mohan [41] to ensure the particles move within the legal search space. In many practical optimization problems, the dimensionality and the location of the global optimum is usually difficult to know *a priori*. It is therefore desirable to have a single boundary condition that can offer a robust and consistent performance for the PSO technique regardless of the problem dimensionality and the location of the global optimum. When the particle exceed a certain dimension of the solution search space, the position of particle will be re-located in the search boundary and its velocity component in the reverse of this dimension and multiplied by a random number (between 0-1).

Mutation scheme is introduced in this algorithm to speed up the convergence when particles are around global optimum. The mutation scheme can also avoid premature convergences in the searching procedure and help the x_{gbest} escape from the local optimal position. It can increase the robustness of the algorithm with full search capabilities to avoid falling into the regional value. More details about the APSO

algorithm can be found in [41]-[42].

The flowchart of the modified APSO is shown in Figure 2. Asynchronous PSO goes through seven procedures as follows:

I. Initialize a starting population: randomly generate a swarm of particles.

II. Calculate the *E* fields by a home-made FDTD code.

III. Evaluate the population using cost function: the asynchronous PSO algorithm evaluates the cost function (3) for each individual in the population.

IV. Find x_{pbest} and x_{gbest}.

V. Mutation scheme: the particle swarm optimization algorithm has been shown to converge rapidly during the initial stages of a global search, but when around the global optimum, the search can become very slow. For the reason, mutation scheme is leaded into asynchronous PSO. As shown in Figure 2, there is an additional competition between the x_{gbest} and $x_{gbest_{mu}}$. The current x_{gbest} will be replaced by the $x_{gbest\,mu}$ if the $x_{gbest\,mu}$ is better than the current x_{gbest}. The $x_{gbest\,mu}$ is generated by following way:

$$X_{gbest_{mu}} = \begin{cases} X_{gbest} - \varphi_3 \cdot \left[c_3 - (c_3 - c_4) \cdot \dfrac{k}{k_{\max}} \right] \cdot (x_{\max} - x_{\min}), & if \quad \varphi_{mu} < 0.5 \\ X_{gbest} + \varphi_3 \cdot \left[c_3 - (c_3 - c_4) \cdot \dfrac{k}{k_{\max}} \right] \cdot (x_{\max} - x_{\min}), & if \quad \varphi_{mu} \geq 0.5 \end{cases} \tag{6}$$

where c_3 and c_4 are the scaling parameter. φ_3 and φ_{mu} are both the random numbers between 0 and 1. k is the current iteration

number. k_{max} is the maximum iteration number. x_{max} and x_{min} are the upper limit and lower limit of the search space, respectively.

VI. Update the velocity and position.

VII. Stop the process and print the best individual if the termination criterion is satisfied; else, go to step 2.

III. NUMERICAL RESULTS

As shown in Figure 1, the problem space is divided in 68×68 grids with the grid size $\Delta x = \Delta y$ =5.95mm. The inhomogeneous dielectric cylinder is buried in a lossless a slab medium($\sigma_1 = \sigma_2 = \sigma_3 = 0$). The transmitters and receivers are placed in free space above the inhomogeneous dielectric slab. The permittivities in region 1, region 2 and region 3 are characterized by $\varepsilon_1 = \varepsilon_0$, $\varepsilon_2 = 8\varepsilon_0$ and $\varepsilon_1 = \varepsilon_0$, respectively, while the permeability μ_0 is assumed for each region, i.e., only non-magnetic media are concerned here. The cylindrical object is illuminated by a transmitter at two different positions, N_i=2, which are located at (154.7mm, 440.3mm) and (440.3mm, 440.3mm), respectively. The scattered E fields for each illumination are collected at the five receivers, M=5, which are equally separated by 23.8mm in the x-axis and the first receiver is located at (119mm, 416.5mm). For the representation of the scatterer properties, seven subdivisions are considered along both x and y axis ($R = U = 7$) and axis resulting in 49 equal square cells. There are 49 unknown parameters to retrieve, which include the scatterers permittivities distribution. The search range of unknowns for permittivity

is chosen from 1.0 to 6.0, determined by the prior knowledge of the object. The related coefficients of the APSO are set below. The learning coefficients c_1 and c_2 are set to 2.8 and 1.3[42]-[43], respectively. The mutation probability is 0.4. Moreover, the relative mean square error of the reconstructed data profile is defined as

$$err = \left[\sum_{i=1}^{N} \left| \Delta \tau_i \right|^2 \Big/ \sum_{i=1}^{N} \left| \tau_i^{exact} \right|^2 \right]^{1/2} \times 100\% \tag{7}$$

where τ_i^{exact} and $\Delta \tau_i$, respectively, denote the exact value of the relative permittivity of the *i*th cell and the difference between the reconstructed and exact values. Reconstruction is carried out on an Intel PC (2.83 GHz/ 2GB memory /500 GB HD). The software is developed on FORTRAN VISION 6.0 in WINDOWS XP system environment. In our simulation, the typical CPU time for 1000 generations is about 4 hours on a home-made Fortran program that runs on an Intel PC (3.4 GHz/ 4G memory /500G).

In the first example, we consider a practical case to detect water buried in the wall, as shown in Fig. 3(a). The whole problem space is considered. The reconstructed error is 27.02 %. From Fig. 3(b), we conclude that the water in the wall is detectable by APSO.

In the second example, let us consider a crisscross-like object, as shown in Fig. 4(a). The relative permittivity of the crisscross axis is 4.5 with four leaves of 2.5. The reconstructed error is 3.89 %. Fig. 4(b) shows that it is clear that the reconstructed result is good by APSO.

In the third example, we consider an X-like object, as shown in Fig. 5(a). The permittivity of the crisscross axis is 4.5 with four leaves of 2.5.

The reconstructed error is 3.09 %. Again, Fig. 5(b) shows it is seen that good reconstruction is achieved by APSO.

In the fourth example, we report on multi-inhomogeneous dielectric objects buried in a lossy slab medium ($\sigma = 2\times10^{-3}$ s/m), as shown in Fig. 6(a). The reconstructed error is 9.68 %, as shown in Fig. 6(b). It is clear that the reconstruction error is less well for the inhomogeneous dielectric objects with high permittivity. However, we can see that reconstruction is better for the illuminated side than that obtained for the backside.

In the last example, to test the problem of reference [33], we have conducted the following studies: a two dimensional inhomogeneous dielectric cylinder buried in half space and slab medium, respectively. Bulges object of $\varepsilon_3 = 3.5$, surrounding area of the object is 2.5, as shown in Fig. 7(a). The reconstructed result is shown in Fig. 7(b) and Fig. 7(c), respectively. The reconstructed error is 2.48 % and 2.61% in slab medium and half space, respectively. It is found that APSO is suitable for inverse scattering problem whether inhomogeneous dielectric cylinders buried in half or slab medium.

From last four examples, we conclude that, in the case of noisy free data, the relative reconstruction errors for all parameters are lower than 10%. In order to investigate the sensitivity of the imaging algorithm against random noise, the additive white Gaussian noise of zero mean with standard deviation σ_g is added into the recorded scattered electric fields to mimic the measurement errors for examples 2 to 4. The signal to noise ratio (SNR) is defined as:

$$SNR = 10\log_{10}\frac{\sum_{n=1}^{Ni}\sum_{m=1}^{Mi}\sum_{b=0}^{B}\left|E_z^{\exp}(n,m,b\Delta t)\right|^2}{\sigma_g^2(N_i)(M_i)(B)} \quad (8)$$

Figure 8 shows the reconstructed results for the cylinder under the condition that the recorded scattered fields are contaminated by noise, of which the SNR includes 40dB, 30dB, 20dB, 10dB and 3dB. It is observed that good reconstruction can be obtained when the SNR is above 10dB.

IV. CONCLUSION

In this paper, the time domain inverse scattering of inhomogeneous dielectric cylinders of arbitrary cross section in three layer space is investigated. By combining the FDTD method and the APSO scheme, good reconstructed results are obtained. Through the APSO scheme, dielectric constant of the object can be successfully reconstructed even when the dielectric constant is relatively large even with lossy or lossless surrounding media. The effects of noise on microwave imaging are examined, and good reconstruction has been obtained even in the presence of white Gaussian noise in experimental data.

REFERENCES

[1] M. Dehmollaian, K. Sarabandi, “Refocusing Through Building Walls Using Synthetic Aperture Radar,” *IEEE Transactions on Geoscience and Remote Sensing*, vol. 46, pp. 1589-1599, 2008.

[2] F. Soldovieri, F. Ahmad and R. Solimene, “Validation of Microwave Tomographic Inverse Scattering Approach via Through-the-Wall Experiments in Semicontrolled Conditions,” *IEEE Transactions Geoscience and Remote Sensing*, Vol. 8, No. 1, pp.123 - 127, Jan. 2011.

[3] A. Massa, M.Pastorino, A. Rosani and M. Benedetti “A Microwave Imaging Method for NDE/NDT Based on the SMW Technique for the Electromagnetic Field Prediction,” *IEEE Transactions on Instrumentation and Measurement*, Vol. 55, No. 1, pp. 240 - 247, Feb. 2006.

[4] M. Benedetti, D. Lesselier, M. Lambert, and A. Massa, “Multiple-Shape Reconstruction by Means of Multiregion Level Sets,” *IEEE Transactions Geoscience and Remote Sensing*, Vol. 48, No. 5, pp.2330 - 2342, May. 2010.

[5] A. Randazzo, K. M. Donnell and Y. S. Lee “Microwave and Millimeter-Wave Sensors, Systems, and Techniques for Electromagnetic Imaging and Materials Characterization,” *International Journal of Microwave Science and Technology*, Vol. 2012, 132136, 2012.

[6] A. Randazzo “Swarm Optimization Methods in Microwave

Imaging," *International Journal of Microwave Science and Technology*, Vol. 2012, 491713, 2012.

[7] M. Pastorino and A. Randazzo "Buried Object Detection by an Inexact Newton Method Applied to Nonlinear Inverse Scattering," *International Journal of Microwave Science and Technology*, Vol. 2012, 637301, 2012.

[8] M. Brignone, G. Bozza, A. Randazzo, M. Piana, and M. Pastorino, "A Hybrid Approach to 3D Microwave Imaging by Using Linear Sampling and ACO", *IEEE Transactions on Antennas and Propagation*, vol. 56, p. 3224–3232, 2008.

[9] C. H. Sun, C. C. Chiu, and C. H. Chen "Time Domain Microwave Imaging for a Metallic Cylinder by Using Evolutionary Algorithms," *Imaging Science Journal*, vol. 61, pp. 3–12, Jan. 2013.

[10] C. C. Chiu and C. H. Sun "Through-Wall Imaging for a Metallic Cylinder," *Nondestructive Testing and Evaluation*, vol. 28, pp. 72–81, Jan. 2013.

[11] D. Colton and R. Kress, *Inverse Acoustic and Electromagnetic Scattering Theory*, Springer-Verlag, New York, 1992.

[12] M. Moghaddam, W. C. Chew, and M. Oristaglio, "A Comparison of the Born iterative method and Tarantola's method for an electromagnetic time-domain inverse problem," *International Journal of Imaging Systems and Technology*, vol. 3, pp. 318-333, 1991.

[13] W. H. Weedon, " *Broadband microwave inverse scattering: Theory*

and experiment," Ph.D. dissertation, University of Illinois at Urbana-Champaign, 1994.

[14] T. Moriyama, Z. Meng, and T. Takenaka, "Forward-backward time-stepping method combined with genetic algorithm applied to breast cancer detection", *Microwave and Optical Technology Letters*, Vol. 53, No. 2, pp.438-442, 2011.

[15] D. S. Weile and E. Michielssen, "Genetic algorithm optimization applied to electromagnetics: a review ," *IEEE Transactions on Antennas and Propagation*, Vol. 45, No. 3, pp. 343- 353, Mar. 1997.

[16] J. Robinson and Y. Rahmat-Samii, "Particle swarm optimization in electromagnetics," *IEEE Transactions on Antennas and Propagation*, Vol. 52, No. 3, pp. 397–407, Feb. 2004.

[17] P. Rocca, G. Oliveri, and A. Massa,"Differential Evolution as Applied to Electromagnetics ," *IEEE Antennas and Propagation Magazine*, Vol. 53, No. 1, pp. 38–49, May. 2011.

[18] C. H. Sun, C. L. Liu, K. C. Chen, C. C. Chiu, C. L. Li, and C. C. Tasi, "Electromagnetic Transverse Electric Wave Inverse Scattering of a Partially Immersed Conductor by Steady-State Genetic Algorithm," *Electromagnetics.* Vol. 28, No. 6, pp. 389-400, Aug. 2008.

[19] C. H. Sun, C. L. Li, C. C. Chiu and C. H. Huang, "Time Domain Image Reconstruction for a Buried 2D Homogeneous Dielectric Cylinder Using NU-SSGA.", *Research in Nondestructive Evaluation*, Vol. 22, No.1, pp. 1-15, Jan. 2011.

[20] A. Saeedfar, and K. Barkeshli, “Shape reconstruction of three-dimensional conducting curved plates using physical optics, number modeling, and genetic algorithm, ” *IEEE Transaction on Antennas and Propagation,* Vol. 54, No. 9, 2497-2507, Sep. 2006.

[21] R A. Wildman and D S. Weile, “Greedy Search And A Hybrid Local Optimization/Genetic Algorithm For Tree-Based Inverse Scattering,” *Microwave and Optical Technology Letters,* Vol. 50, No. 3, pp. pp. 822-825, Mar. 2008.

[22] I.T. Rekanos, and A. Trochidis, "Shape reconstruction of two-dimensional acoustic obstacle using particle swarm optimization," *Acta Acustica United with Acustica*, vol. 93, no. 6, pp. 917-923, Nov.-Dec. 2007.

[23] C. C. Chiu, C. H. Sun and Y. S. Fan “Shape Reconstruction of 2-D Perfectly Conducting Cylinder Targets Using the Particle Swarm Optimization.” *Imaging Science Journal.* Vol. 60, No 2, pp. 83-89, Apr. 2012.

[24] C. H. Sun, C. C. Chiu and C. L. Li, “Time-Domain Inverse Scattering of a Two- dimensional Metallic Cylinder in Slab Medium Using Asynchronous Particle Swarm Optimization.”, *Progress In Electromagnetic Research M.* PIER M Vol. 14, pp. 85-100. Aug. 2010.

[25] C. C. Chiu, C. H. Sun and W. L. Chang “Comparison of Particle Swarm Optimization and Asynchronous Particle Swarm Optimization for Inverse Scattering of a Two- Dimensional Perfectly Conducting Cylinder.”, *International Journal of Applied Electromagnetics and*

Mechanics Vol. 35, No.4, pp. 249-261,Apr. 2011.

[26] I. T. Rekanos, “Shape Reconstruction of a Perfectly Conducting Scatterer Using Differential Evolution and Particle Swarm Optimization,” *IEEE Transactions on Geoscience and Remote Sensing*, Vol. 46, no. 7, pp. 1967-1974, 2008.

[27] C. H. Sun, C. C. Chiu, C. L. Li, and C. H. Huang, “Time Domain Image Reconstruction for Homogenous Dielectric Objects by Dynamic Differential Evolution,” *Electromagnetics.* Vol. 30, No. 4, pp. 309-323, May. 2010.

[28] C. H. Sun, C. C. Chiu, W. Chien and C. L. Li, “Application of FDTD and Dynamic Differential Evolution for Inverse Scattering of a Two-Dimensional Perfectly Conducting Cylinder in Slab Medium”, *Journal of Electronic Imaging.* Vol. 19, 043016, Dec. 2010.

[29] C. H. Sun and C. C. Chiu, “Inverse Scattering of Dielectric Cylindrical Target Using Dynamic Differential Evolution and Self-Adaptive Dynamic Differential Evolution,” *International Journal of RF and Microwave Computer-Aided Engineering,* Vol. 23, Issue 5, pp. 579–585, Sept. 2013.

[30] A. Massa, M. Pastorino, and A. Randazzo, “Reconstruction of two-dimensional buried objects by a differential evolution method”, *Inverse Problems*, vol. 20, p. S135–S150, 2004.

[31] A. Qing, “Dynamic differential evolution strategy and applications in electromagnetic inverse scattering problems”, *IEEE Transactions on Geoscience and Remote Sensing*, Vol. 44, No. 1, pp.116-125, January, 2006.

[32] A. Semnani, I. T. Rekanos, M. Kamyab, and T. G. Papadopoulos,

"Two-Dimensional Microwave Imaging Based on Hybrid Scatterer Representation and Differential Evolution," *IEEE Trans. Antennas Propag.*, vol. 58, no. 10, pp. 3289–3298, Oct. 2010.

[33] C. C. Chiu and S. J. Chen "Time Domain Inverse Scattering of Buried Inhomogeneous Dielectric Cylinders." *Journal of Nondestructive Evaluation.* Vol.31, No.2, pp. 128-139, May. 2012.

[34] T. G. Papadopoulos and I. T. Rekanos "Time-Domain Microwave Imaging of Inhomogeneous Debye Dispersive Scatterers." *IEEE Trans. Antennas Propag.*, vol. 60, no. 2, pp. 1197–1202, Feb. 2012.

[35] C. L. Li, C. W. Liu, and S. H. Chen, "Optimization of a PML Absorber's Conductivity Profile using FDTD," *Microwave and Optical Technology Letters.*, vol. 37, pp. 380-383, 2003.

[36] J. Kennedy and R. C. Eberhart, "Particle swarm optimization," *Proceedings of the IEEE International Conference on Neural Network*, 1942-1948, 1995.

[37] J. F. Kennedy, R. C. Eberhart, and Y. Shi, Swarm intelligence. San Francisco: Morgan Kaufmann Publishers, 2001.

[38] M. Benedetti, R. Azaro, and Andrea Massa, "Memory Enhanced PSO-Based Optimization Approach for Smart Antennas Control in Complex Interference Scenarios," *IEEE Transactions on Antennas and Propagation*. Vol. 56, No. 7, pp. 1939-1947, Jul. 2008.

[39] Jin, N. and Y. Rahmat-Samii, "Advances in particle swarm optimization for antenna designs: Real-number, binary, single-objective and multiobjective implementations," *IEEE Transactions on Antennas and Propagation*, Vol. 55, No. 3, 556-567,

2007.

[40] M. Clerc, “The swarm and the queen: towards a deterministic and adaptive particle swarm optimization,” *Proceedings of Congress on Evolutionary Computation*, Washington, DC, pp 1951-1957, 1999.

[41] T. Huang, A. S. Mohan, “A Hybrid Boundary Condition for Robust Particle Swarm. Optimization,” *IEEE Antennas and Wireless Propagation Letters*, vol. 4, pp.112-117, 2005.

[42] C. C. Chiu, C. H. Sun, C. L. Li and C. H. Huang, “Comparative Study of Some Population-based Optimization Algorithms on Inverse Scattering of a Two- Dimensional Perfectly Conducting Cylinder in Slab Medium,” *IEEE Transactions on Geoscience and Remote Sensing*, vol. 51, pp. 2302–2315, Apr. 2013.

[43] A. Carlisle and G. Dozier, “An Off-The-Shelf PSO,” *Proceedings of the 2001 Workshop on Particle Swarm Optimization*, pp.1-6, 2001.

Caption

Fig. 1 Geometry for the inverse scattering of a dielectric cylinder buried in a slab medium.

Fig. 2 Flowchart for the asynchronous particle swarm optimization

Fig. 3(a) Original permittivity distribution

Fig. 3(b) Reconstructed permittivity distribution with a 27.02% error

Fig. 4(a) Original permittivity distribution

Fig. 4(b) Reconstructed permittivity distribution with a 3.89% error

Fig. 5(a) Original permittivity distribution

Fig. 5(b) Reconstructed permittivity distribution with a 3.09% error

Fig. 6(a) Original permittivity distribution

Fig. 6(b) Reconstructed permittivity distribution with a 9.68% error

Fig. 7(a) Original permittivity distribution

Fig. 7(b) Reconstructed permittivity distribution buried in slab medium

Fig. 7(c) Reconstructed permittivity distribution buried in half space

Fig. 8 Reconstruction error as function of SNR by APSO

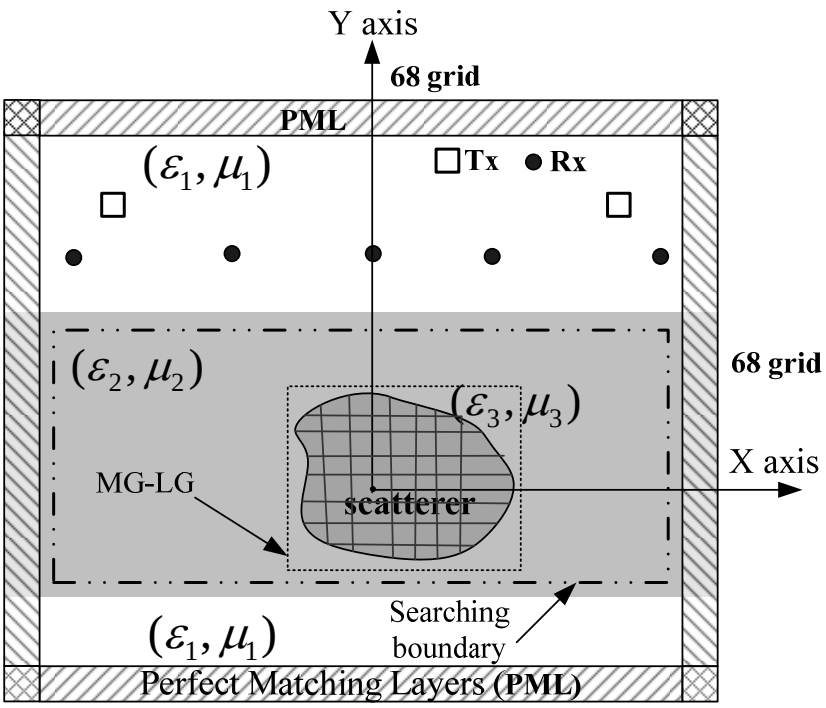

Fig. 1 Geometry for the inverse scattering of a dielectric cylinder buried in a slab medium

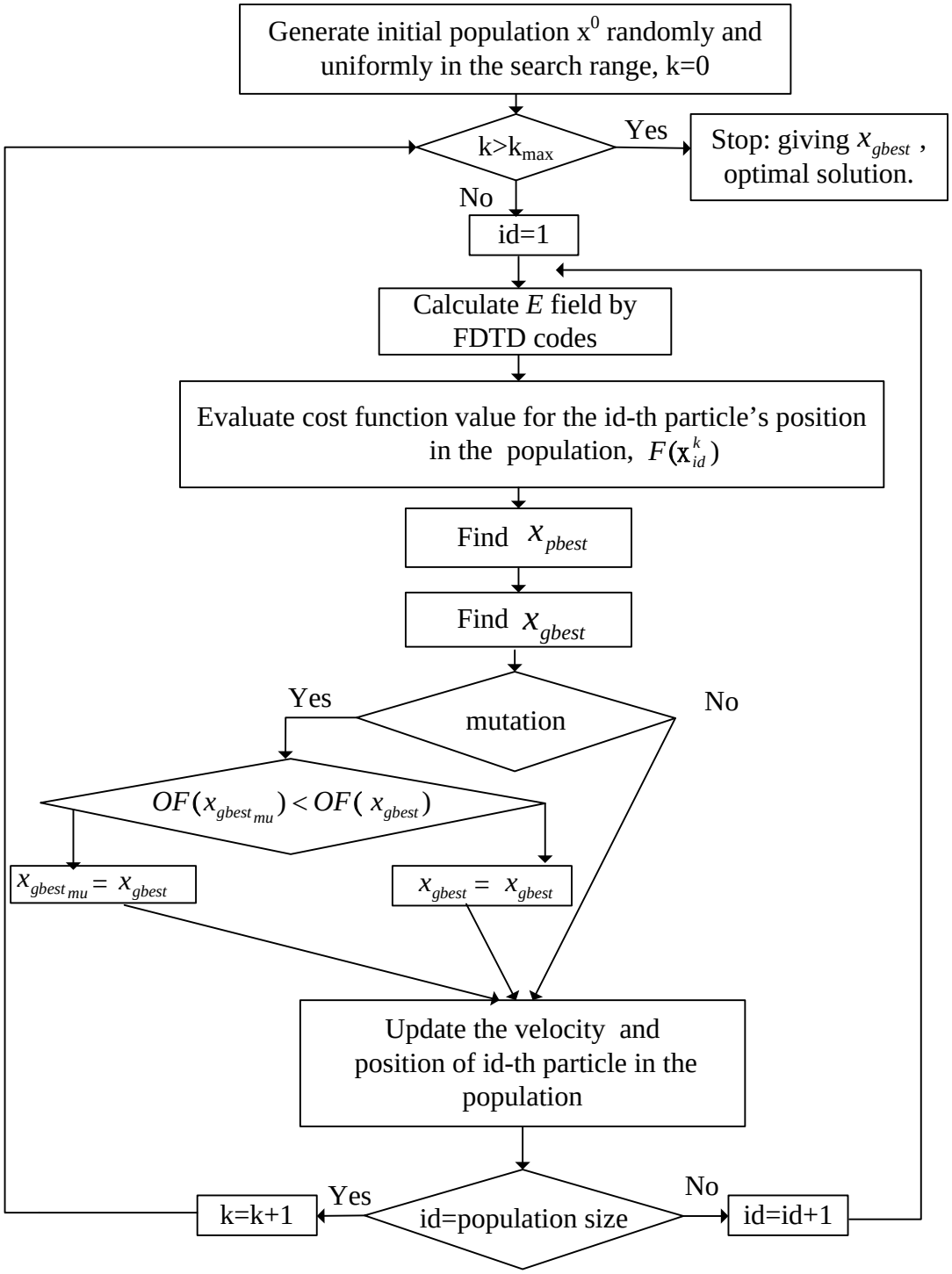

Fig. 2 Flowchart for the asynchronous particle swarm optimization

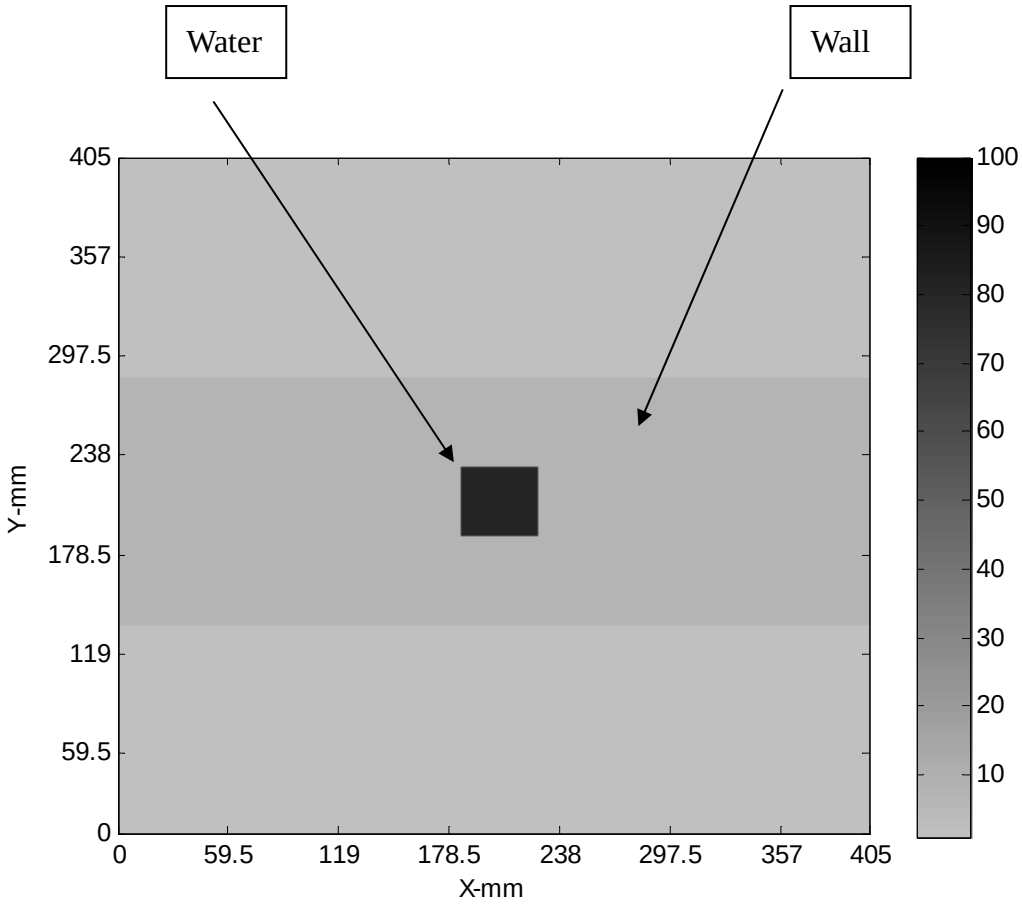

Fig. 3(a) Original dielectric constant

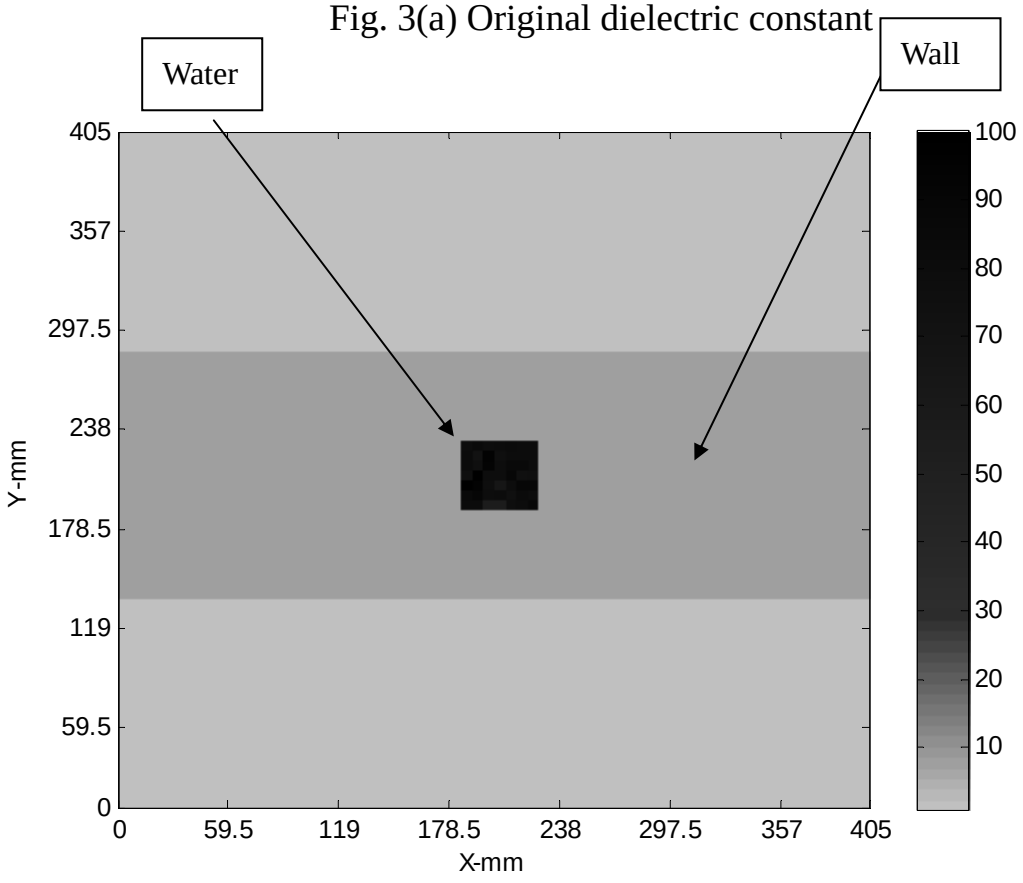

Fig. 3(b) Reconstructed permittivity distribution with a 27.02% error

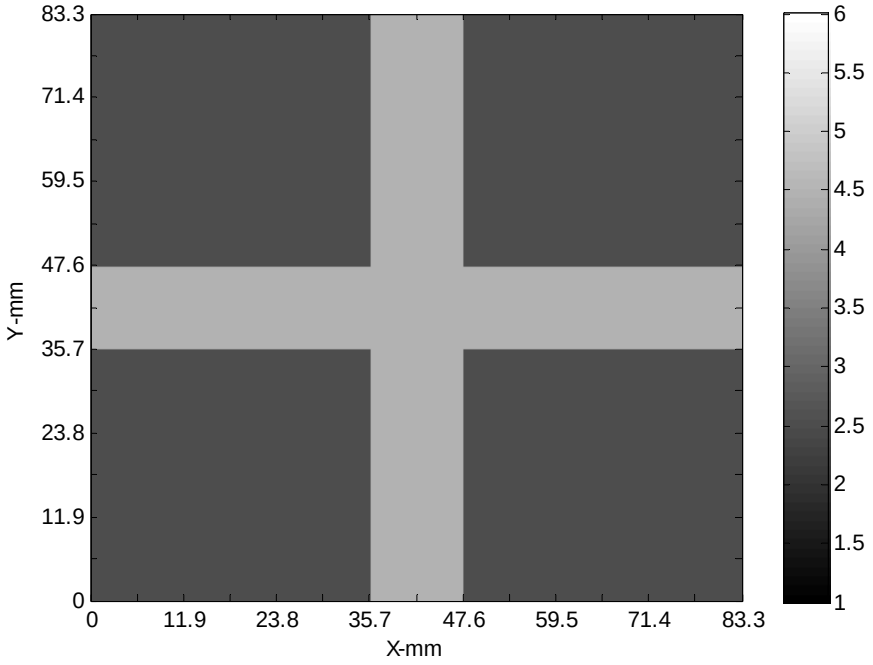

Fig. 4(a) Original dielectric constant

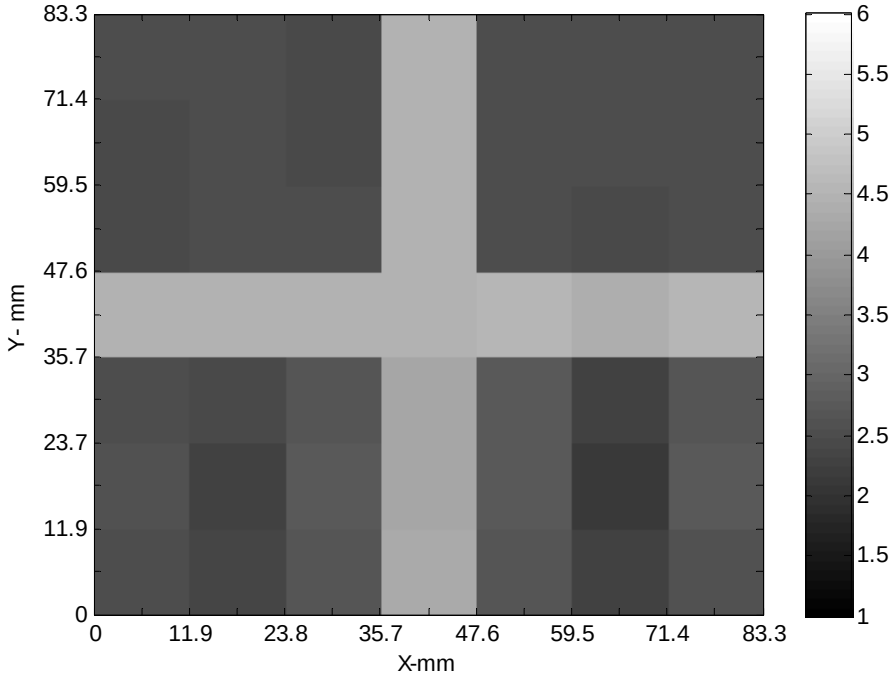

Fig. 4(b) Reconstructed permittivity distribution with a 3.89% error

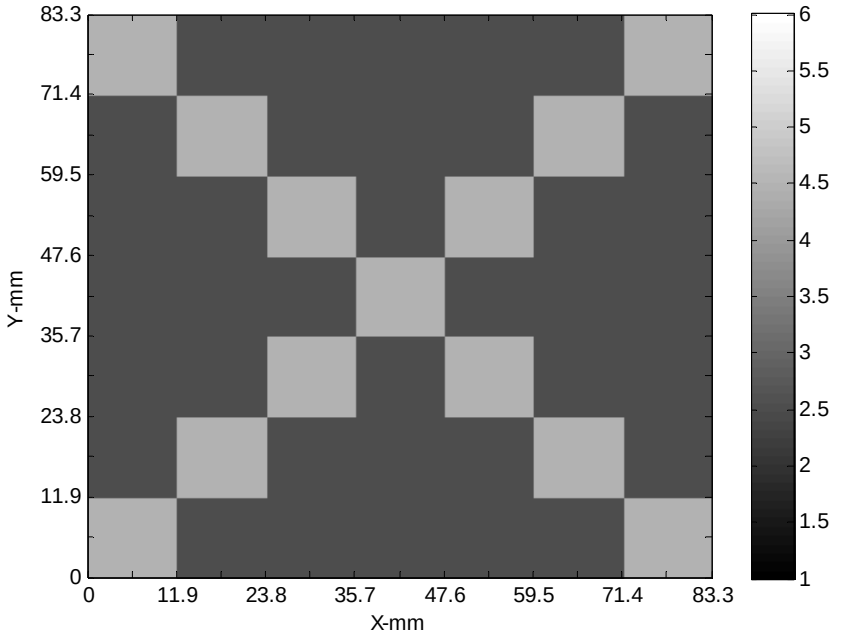

Fig. 5(a) Original dielectric constant

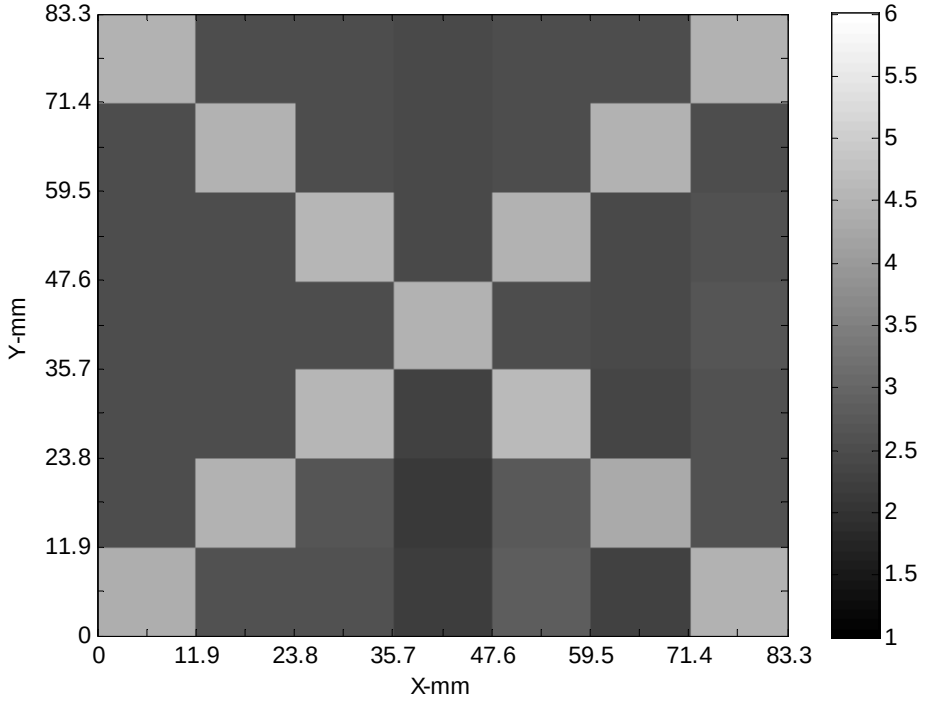

Fig.5 (b) Reconstructed permittivity distribution with a 3.09% error

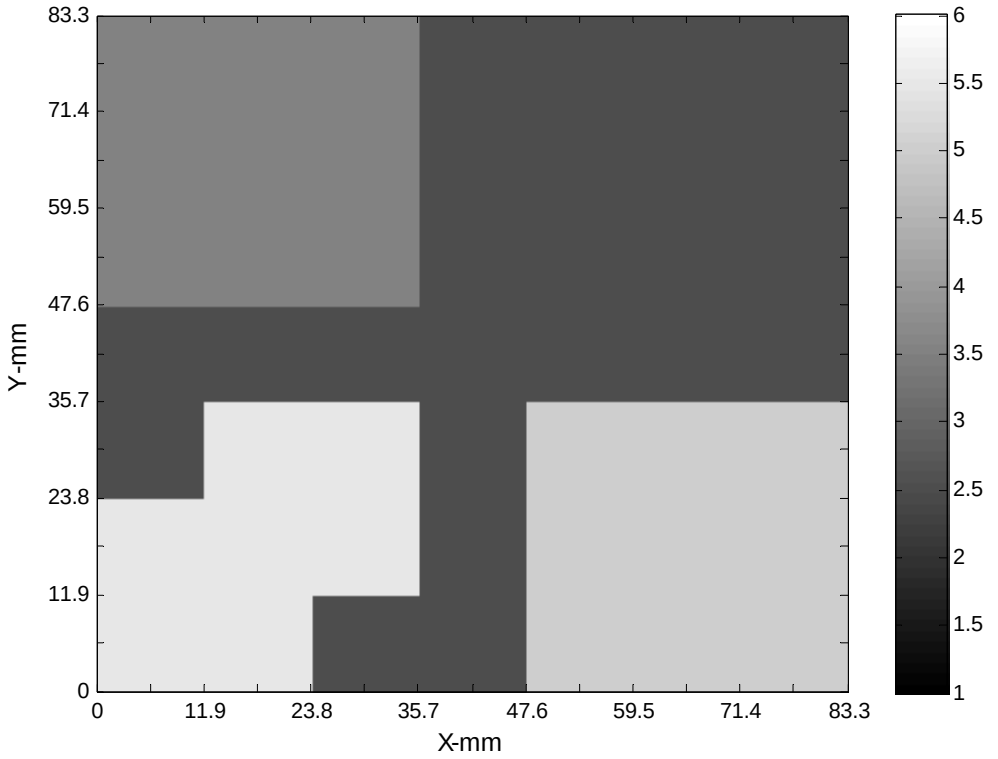

Fig. 6(a) Original dielectric constant

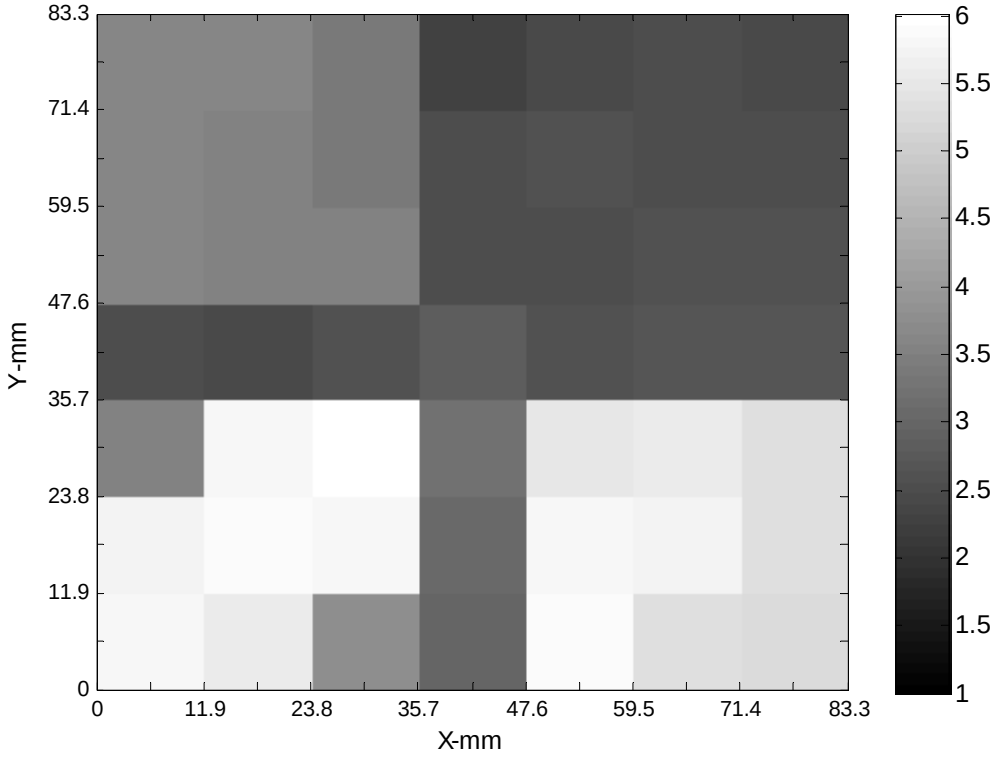

Fig.6 (b) Reconstructed permittivity distribution with a 9.68% error

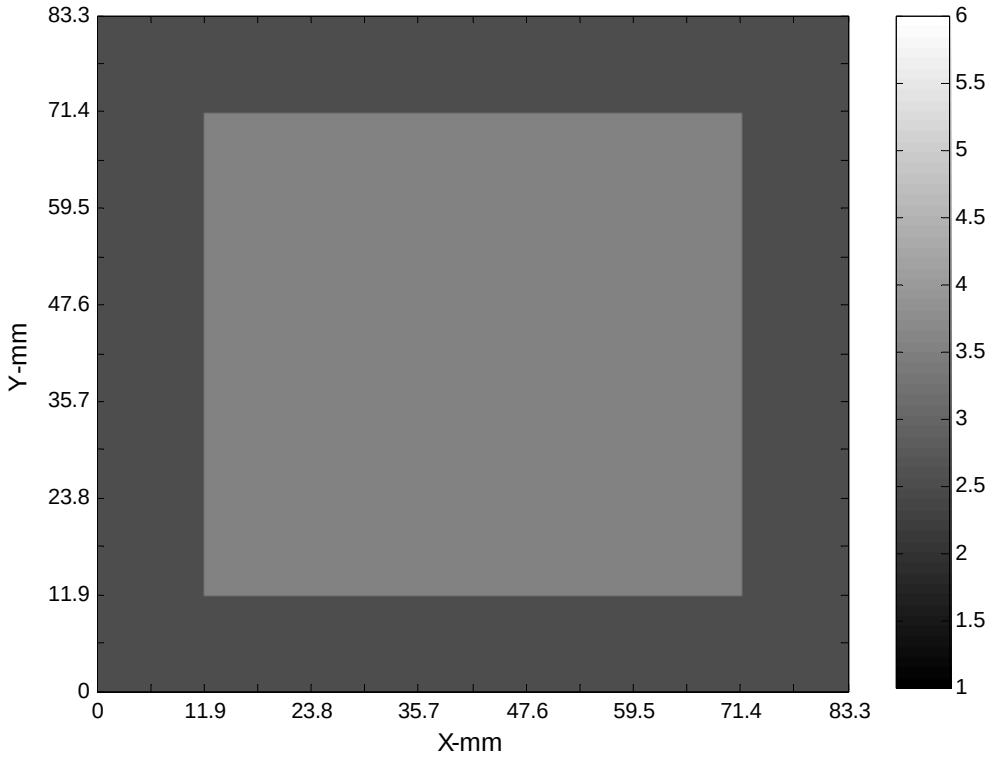

Fig. 7(a) Original dielectric constant

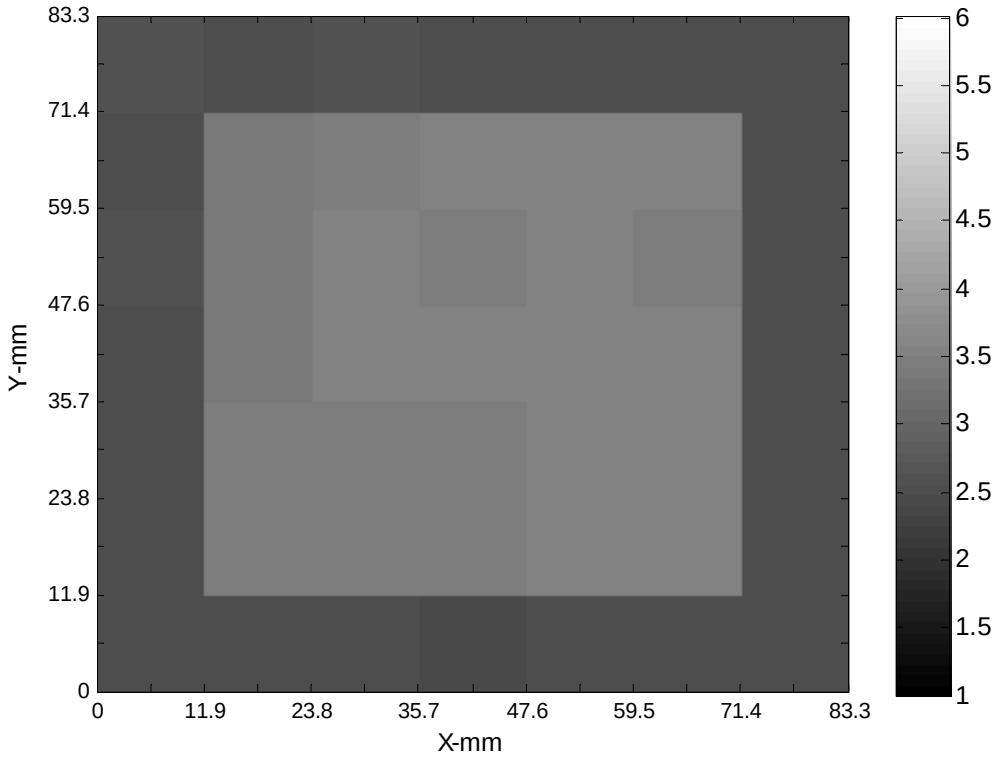

Fig.7 (b) Reconstructed permittivity distribution buried in slab medium

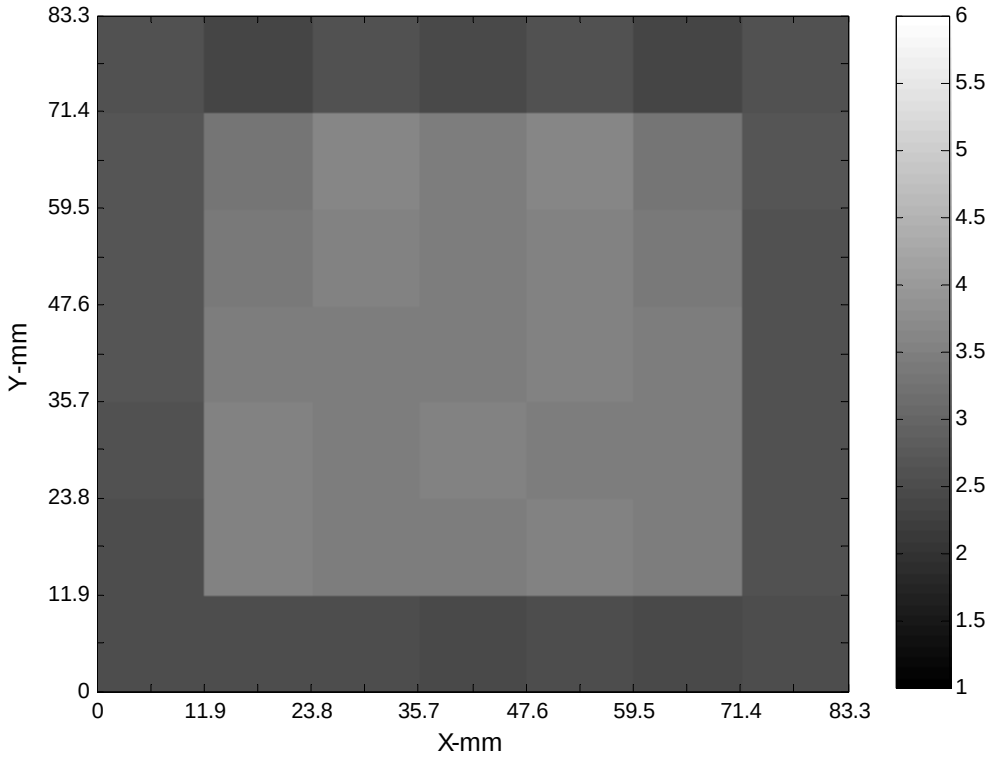

Fig.7 (c) Reconstructed permittivity distribution buried in half space

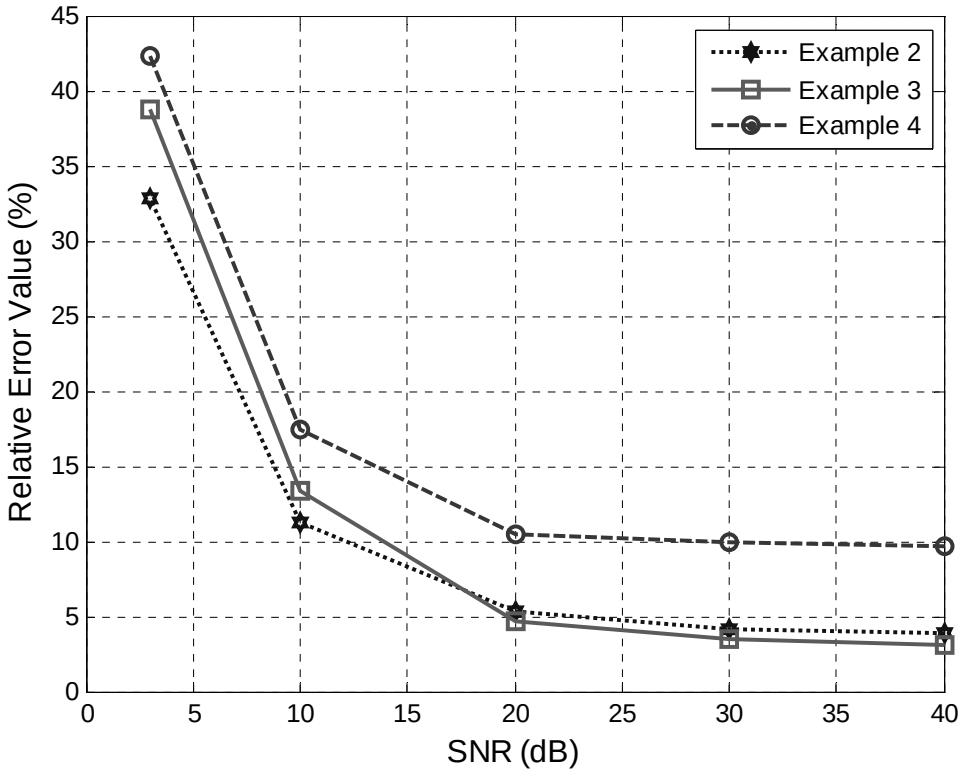

Fig 8.Reconstruction error as function of SNR by APSO